DIRECT CHANNEL EFFECTS IN NONDIFFRACTIVE SCATTERING*

J.A.J. Matthews
Stanford Linear Accelerator Center
Stanford University, Stanford, California 94305

ABSTRACT

Direct channel or absorption effects are first considered for π exchange reactions, and in particular for $\pi N \rightarrow \rho N$. The discussion is then restricted to nondiffractive pseudoscalar-meson baryon scattering reactions, where only two helicity amplitudes define the scattering process. The 6 GeV/c πp amplitude analyses are reviewed; energy dependences of various features of the data are then studied to obtain a qualitative understanding of the energy trends of the helicity amplitudes. The relation of these results to $\pi\pi$ analyses is discussed.

I. INTRODUCTION

Many features of two body and quasi-two body scattering data are most easily understood under the general title of direct channel or absorption effects. The most familiar examples are momentum transfer dependent features of the scattering data: the "anomalous" forward peaks in certain π exchange differential cross sections[1-5] and the crossover phenomena in elastic scattering.[6,7] However, absorption may also result in energy or particle dependent variations in the data.

In the present talk we investigate the general features of absorption by systematically studying data over a large energy interval and in several different reactions. The relation of our observations to $\pi\pi$ scattering analyses is emphasized.

The qualitative ideas associated with absorption are introduced in Sec. II using the familiar reaction $\pi N \rightarrow \rho N$. The study is then restricted in Sec. III to the simpler pseudoscalar-meson baryon scattering reactions, described by two helicity amplitudes, and having only natural parity exchanges in the t channel. Only nondiffractive reactions are considered.

The πp amplitude analyses at 6 GeV/c are discussed first, providing an introduction to the t dependence of the scattering amplitudes. To extend the results of the amplitude analyses, data in several reactions are studied to determine qualitative trends in the energy dependences of the scattering amplitudes. In particular data in πp and Kp reactions are contrasted to reveal possible direct channel effects.

The observations are summarized in Sec. IV.

II. INTRODUCTION TO ABSORPTION

For many years absorption has been known to provide a simple explanation of the $\pi^- p \to \rho^0 n$ data at small values of momentum transfer. Historically, simple one pion exchange (OPE) failed in ρ^0 production, predicting $\rho_{00}^{GH} = 1$. In contrast the Gottfried-Jackson OPE plus absorption model[8] successfully reproduced the ρ^0 differential cross section and density matrix elements.

More recently it has been emphasized that in π exchange reactions an unambiguous signature of absorption occurs for $-t < m_\pi^2$. As discussed by Kane,[9] ρ_{00}^{GJ} and $d\sigma/dt$ for ρ^0 production should turn over in the forward direction, but ρ_{11}^H $d\sigma/dt$ should have a sharp forward peak. This has since been observed at 15 GeV/c,[4, 10] see Fig. 1, and more recently at 17 17 GeV/c.[11] Analogous features are seen in the forward cross sections for the reactions $\gamma p \to \pi^+ n$,[1] $p\bar{p} \to n\bar{n}$,[3] and np charge exchange.[2]
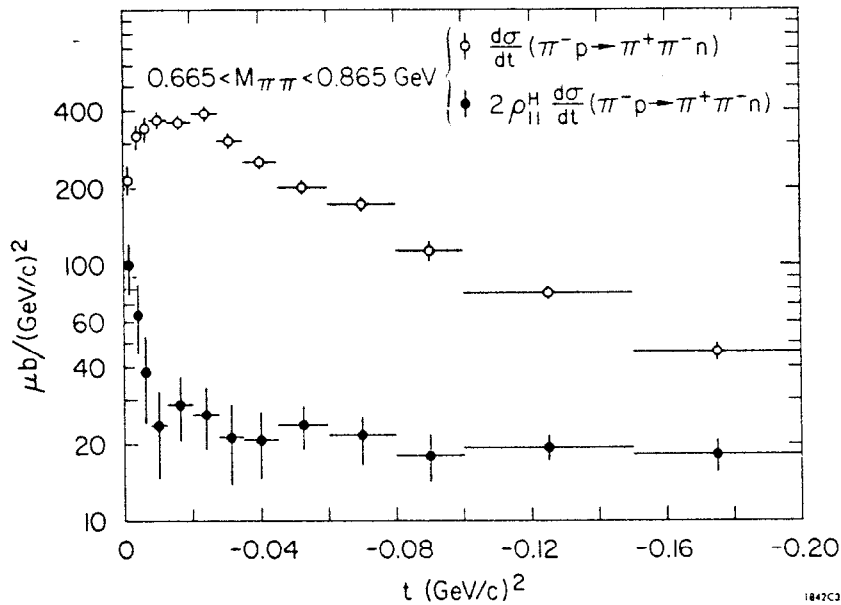

Fig. 1. Differential cross sections from the reaction $\pi^- p \to \rho^0 n$ at 15 GeV/c.

In the absorption model the explanation for this behavior is straightforward. Absorption "smooths" the amplitudes, thus in the forward direction helicity amplitudes possess only the minimal t dependence, $(t_{min} - t)^{\Delta\lambda}$, consistent with conservation of angular momentum. The net helicity flip, $\Delta\lambda$, is defined in the s channel or helicity frame. In the limit of large energies, the dominant π exchange amplitudes flip the nucleon s channel helicity, resulting in π exchange contributions to $\pi N \to \rho N$ of the form:

$$H_{+-}^{\lambda\rho} = f_{\Delta\lambda}(t) \sim \frac{(t_{min} - t)^{\Delta\lambda}}{(t - m_\pi^2)} \tag{1}$$

where λ_ρ is the ρ helicity, and $\Delta\lambda = \lambda_\rho - 1$. For scattering near $t \sim t_{min}$, the $\lambda_\rho = 1$ amplitude dominates yielding $\rho^H_{11} \sim 0.5$ as observed in Fig. 1. A popular model that embodies the features of absorption is the Williams OPE-δ [12] or poor man's absorption model;[13] this has been successfully compared to the high energy ρ^0 production data.[10]

The unique features of the data discussed above are a special argument for absorption however, relying as much on the proximity of the π pole to the physical region as on absorption itself. More generally absorption or geometrical models suggest that s channel helicity amplitudes have the approximate form[4]:

$$f_{\Delta\lambda}(t) \sim J_{\Delta\lambda}(r \sqrt{-t}) \tag{2}$$

where r, the radius in impact parameter space where the amplitude is maximum, is approximately $r \sim 1\,\mathrm{fm} \sim 5\ \mathrm{GeV}^{-1}$. Thus $\Delta\lambda = 0, 1$ amplitudes are predicted to have minima (or zeros) at $-t \sim 0.2,\ 0.6\ \mathrm{GeV}^2$, respectively. The former zero is responsible for the crossover effect in elastic scattering reactions,[7] the latter usually vies with the Regge signature zero as the more basic interpretation for helicity flip amplitudes.

For the reaction $\pi N \to \rho N$, the combination $\rho^H_{00}\ d\sigma/dt$ isolates unnatural parity exchange to leading order in the energy. If A_1 exchange is small[15] then $\rho^H_{00}\ d\sigma/dt$ isolates the π contribution to the single s channel helicity amplitude $f_{\Delta\lambda=1}$. Recent experimental results (Refs. 16–18) suggest that $\rho^H_{00}\ d\sigma/dt$ has a change in t dependence near $-t \sim 0.6$ GeV^2, perhaps even possessing a dip in this momentum transfer region. The most optimistic evidence of this type (Refs. 17, 18) is shown in Figs. 2 and 3.

One explanation for the $\rho^H_{00}\ d\sigma/dt$ data associates only the forward peak with π exchange; this decreases rapidly becoming less than an approximately t independent background near $-t \sim 0.6$ GeV^2.[19] Alternatively the data may suggest that the π amplitude has a minimum near $-t \sim 0.6\ \mathrm{GeV}^2$, similar to the ρ amplitude in $\pi^- p \to \pi^0 n$. For the ρ amplitude the dip in $\pi^- p \to \pi^0 n$ can be interpreted as either an absorption effect (Eq. (2)) or a manifestation of the Regge signature factor:

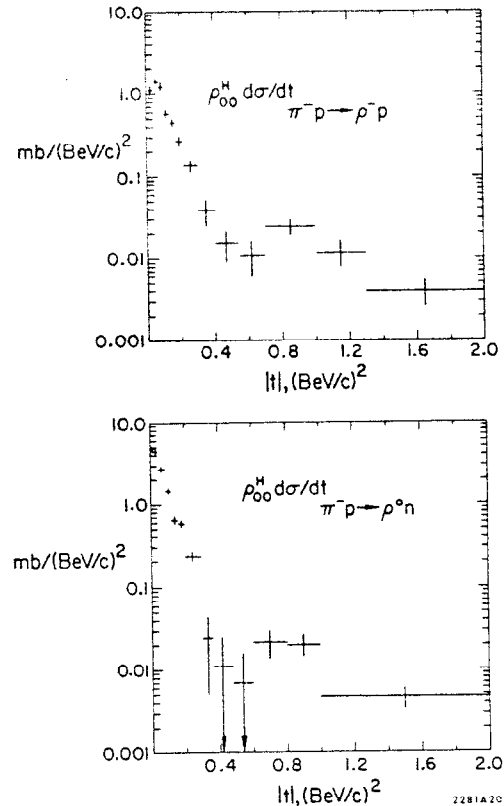$$f_{\Delta\lambda}(t) \sim \tilde{f}(t)\left(1 - e^{-i\pi\alpha_\rho(t)}\right) \tag{3}$$

Fig. 2. Differential cross sections $\rho^H_{00}\ d\sigma/dt$ at 4.42 GeV/c from Ref. 17.

since $\alpha_\rho(t) = 0$ at $-t \sim 0.6$ GeV.[2] However, for π exchange the signature zero should occur at $-t \sim 1.0$ GeV^2, in disagreement with the data. The ρ_{00}^H $d\sigma/dt$ data may therefore provide the first realistic comparison of absorption and Regge model explanations for the structure of helicity flip amplitudes.

III. PSEUDOSCALAR-MESON BARYON SCATTERING

To continue the study of absorption, we now restrict the scope of this talk to nondiffractive pseudoscalar-meson baryon scattering reactions — the simplest class of reactions for which a substantial library of data presently exists. Features of the data will be related to the s channel helicity amplitudes:

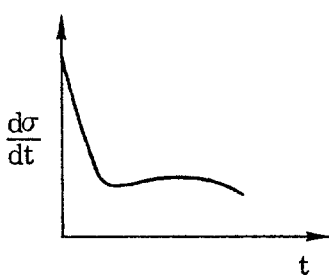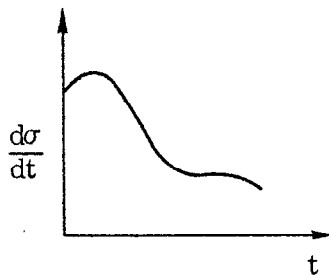$$\text{NONFLIP} \equiv f_{\Delta\lambda=0} \equiv f_{++}$$

and (4)

$$\text{FLIP} \equiv f_{\Delta\lambda=1} \equiv f_{+-}$$
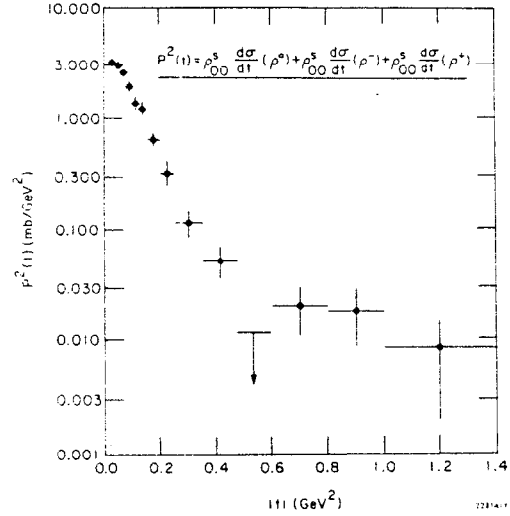
Fig. 3. Combined differential cross sections ρ_{00}^H $d\sigma/dt$ from the three channels $\pi^- p \rightarrow \rho^- p$, $\pi^- p \rightarrow \rho^0 n$ and $\pi^+ p \rightarrow \rho^+ p$ at 6 GeV/c, from Ref. 18.

The amplitudes are briefly reviewed in Table I.

Table I s channel helicity amplitudes

Amplitude	$\|f_{\Delta\lambda}\|^2$	Typical Reactions	Dominant t channel quantum numbers
$f_{\Delta\lambda=0}$	$\frac{d\sigma}{dt}$	$K_L^0 p \rightarrow K_S^0 p$ $\pi p \rightarrow K(\Lambda, \Sigma)$ $\overline{K}p \rightarrow \pi(\Lambda, \Sigma)$	ω^0, K^*, K^{**}, $I_t = 0, \frac{1}{2}$
$f_{\Delta\lambda=1}$	$\frac{d\sigma}{dt}$	$\pi^- p \rightarrow \pi^0 n$ $\pi^- p \rightarrow \eta^0 n$	ρ, A_2, $I_t = 1$

Measurable quantities then have the following forms:

$$\frac{d\sigma}{dt} = |f_{\Delta\lambda=0}|^2 + |f_{\Delta\lambda=1}|^2$$

$$P\frac{d\sigma}{dt} = -2\,\mathrm{Im}\left(f_{\Delta\lambda=0}\,f^*_{\Delta\lambda=1}\right)$$

$$R\frac{d\sigma}{dt} = -\left(|f_{\Delta\lambda=0}|^2 - |f_{\Delta\lambda=1}|^2\right)\cos\theta_{\mathrm{lab}} - 2\,\mathrm{Re}\left(f_{\Delta\lambda=0}\,f^*_{\Delta\lambda=1}\right)\sin\theta_{\mathrm{lab}}$$

$$A\frac{d\sigma}{dt} = \left(|f_{\Delta\lambda=0}|^2 - |f_{\Delta\lambda=1}|^2\right)\sin\theta_{\mathrm{lab}} - 2\,\mathrm{Re}\left(f_{\Delta\lambda=0}\,f^*_{\Delta\lambda=1}\right)\cos\theta_{\mathrm{lab}}$$

$$(5)$$

where P is the polarization normal to the scattering plane, and R, A are measurements of the nucleon polarization in the scattering plane, as shown in Fig. 4.

Having measured a sufficient number of quantities in Eq. (5), the detailed structure of the scattering amplitudes can be determined in a model independent manner. In $\pi N \to \pi N$ for example, there are four complex amplitudes: t channel isospin $I_t=0, 1$ and helicities $\Delta\lambda=0, 1$; for comparison in $\pi N \to \rho N$ there are twelve complex amplitudes: $I_t=0, 1$ and six helicity amplitudes. Such an amplitude analysis for $\pi N \to \pi N$ has recently been possible at 6 GeV/c; the results of the Argonne analysis[20] are shown in Fig. 5. Qualitatively we

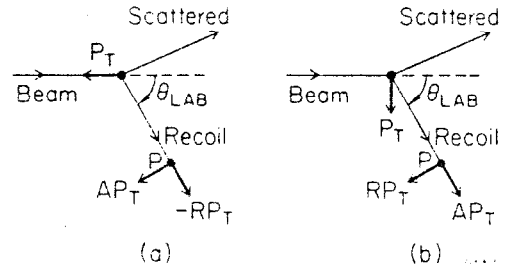

Fig. 4. Scattering geometries for the measurement of the R and A polarization parameters. Initial target polarization, P_T, is in the scattering plane.
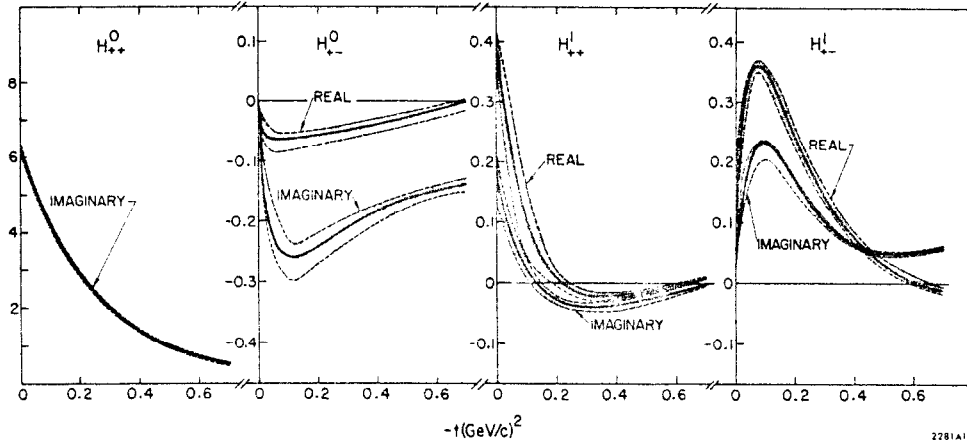

Fig. 5. πN s channel helicity amplitudes, $H^{I_t}_{\Delta\lambda}$, determined at 6 GeV/c from Ref. 20.

observe:

(a) $I_t=0$ amplitudes, since the Pomeron dominates the helicity nonflip (and possibly also the helicity flip) amplitude, no model independent information is obtained for the f^0 exchange amplitudes; and

(b) $I_t=1$ amplitudes, the ρ exchange amplitude is consistent with absorption model predictions for the helicity nonflip amplitude (cf. Eq. (2)), and with absorption or simple Regge model predictions for the helicity flip amplitude (cf. Eqs. (2) and (3)).

To test the sensitivity of these results to possible systematic effects in the data or to different analysis techniques, the Argonne[20] and Saclay[21] solutions are compared in Fig. 6. The agreement is good, except possibly for $-t \gtrsim 0.4$ GeV^2 where some deviations are observed in the $I_t=1$ amplitudes. These amplitudes will be taken therefore as a guide to our further study of meson baryon scattering reactions.
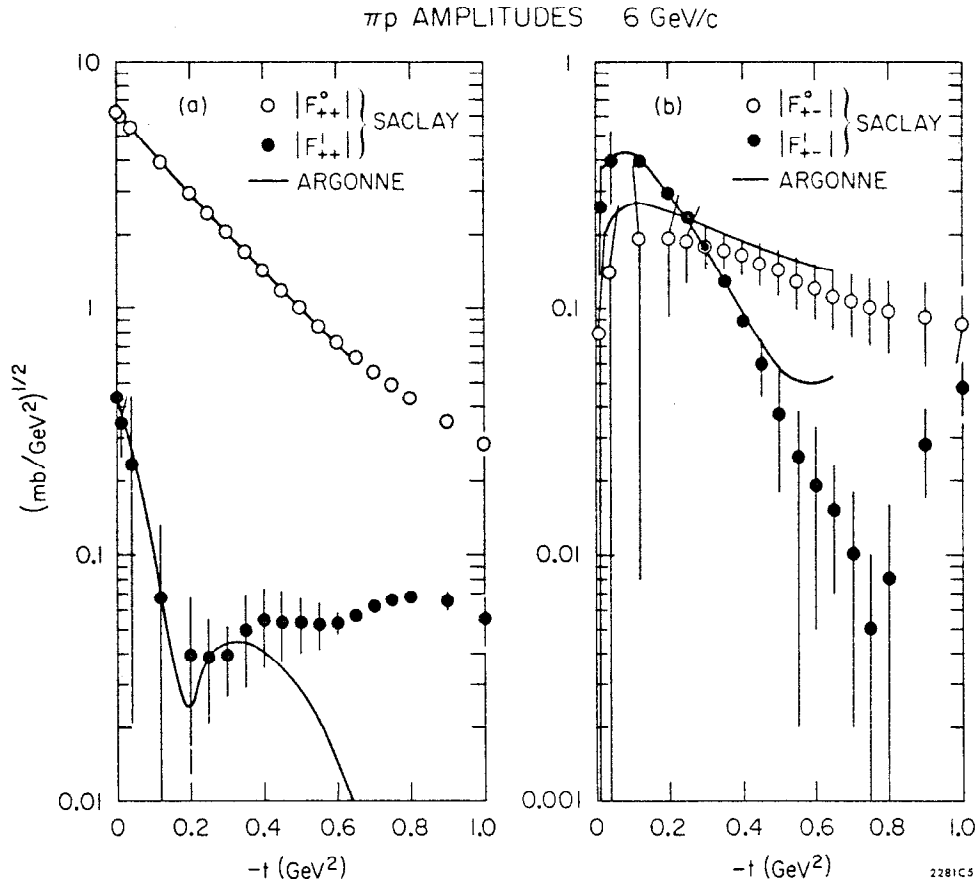
πp AMPLITUDES   6 GeV/c

Fig. 6. Moduli of the 6 GeV/c πN helicity amplitudes from the Argonne analysis, Ref. 20, and the Saclay analysis, Ref. 21.

To extend the results of the 6 GeV/c πN amplitude analyses to different energies and reactions, we now consider six signposts which may lead to qualitative, if not quantitative, extrapolations.

Special Channels

If high energy scattering amplitudes can be described by the t channel exchanges involved, then reactions having only one known t channel exchange should provide the best means to systematize our study of the data. This logic has motivated the many analyses of $\pi^-p \to \pi^0 n$ and $\pi^-p \to \eta^0 n$ reactions; recently data has also begun to accumulate in several new channels:

(a) $K_L^0 p \to K_S^0 p$ — ω^0 exchange dominates the forward cross section;

(b) $K^-p \to \eta^0\Lambda$ — K^* exchange dominates; and

(c) $K^-p \to \eta'\Lambda$ — K^{**} exchange dominates.

These reactions are listed with the "old faithfuls" in Table II.

Table II Special channels of interest

Old faithfuls	New allies	Reaction	SU(3) amplitudes [a]	t channel quantum number exchange
X		$\pi^-p \to \pi^0 n$	$-\sqrt{2}\,V$	ρ
X		$\pi^-p \to \eta_8 n$	$\sqrt{2/3}\,T$	A_2
		$\pi^-p \to \eta_1 n$	$\sqrt{2/3}\,S_T T$	A_2
	X	$K_L^0 p \to K_S^0 p$	$\frac{1}{2}\left[(4F-1)\omega - \rho\right]$ [b] $\equiv (2F-1)V$	$\Big\}\ \omega,\rho$
	X	$K^-p \to \eta_8\Lambda^0$	$-1/6(2F+1)(T+3V)$	$K^*(K^{**})$
	X	$K^-p \to \eta_1\Lambda^0$	$1/3(2F+1)S_T T$	K^{**}

(a) Note that F is defined such that F+D=1, and experimentally $F_{\Delta\lambda=0} \sim 1.25$, $F_{\Delta\lambda=1} \sim 0.25$.

(b) It is assumed that ϕ exchange is negligible, having zero coupling at the nucleon vertex.

The physical states η^0 and η' are dominantly SU(3) octet and singlet components:

$$\eta^0 = \eta_8 \cos\theta - \eta_1 \sin\theta$$

$$\eta' = \eta_8 \sin\theta + \eta_1 \cos\theta$$

where θ is typically in the range $-11 \gtrsim \theta \gtrsim -23°$, the limits of the quadratic and linear SU(3) mass formulae.[22] A compilation[23] of the $K^-p \to (\eta^0, \eta')\Lambda$ data is shown in Fig. 7. The data in the two channels are quite different in structure, and may suggest that absorption differs for vector and tensor exchange reactions.[24]
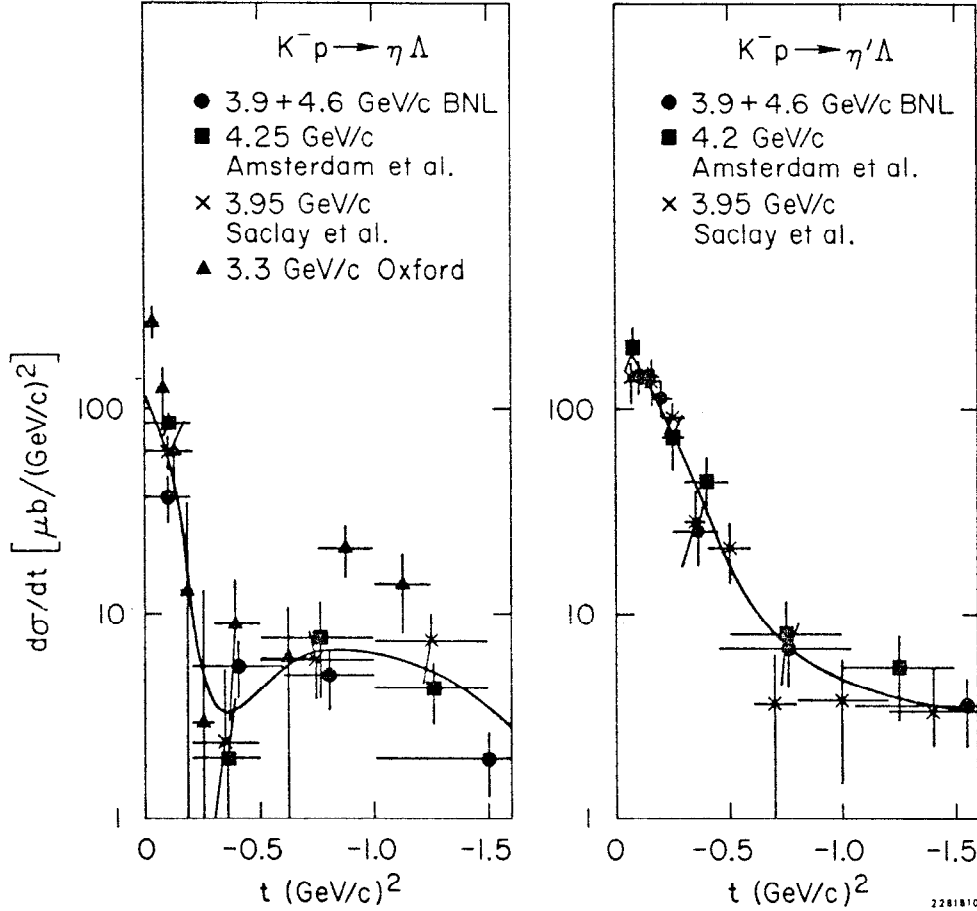

Fig. 7. Compilation of data in the reactions $K^-p \to \eta^0\Lambda$ and $K^-p \to \eta'\Lambda$.

Amplitude zeros and minima in differential cross sections

An intriguing feature of many differential cross sections is the existence of minima at approximately fixed values of t (or u), independent of the reaction energy. This is shown in Figs. 8 and 9 where the locations of minima in the differential cross sections for $\pi^-p \to \pi^0n$ and $\pi^-p \to \eta^0n$ are recorded,[25] fixed t dips are observed at $-t \sim 0.55$ GeV^2 and $-t \sim 1.65$ GeV^2 respectively.

Similar fixed t dependences are found in the contributions of s channel resonances to the imaginary parts of the s channel helicity amplitudes. This is shown for πp scattering[26] in Fig. 10, where the locations of the first zero in the contribution of the dominant resonances to helicity flip and nonflip amplitudes are plotted.
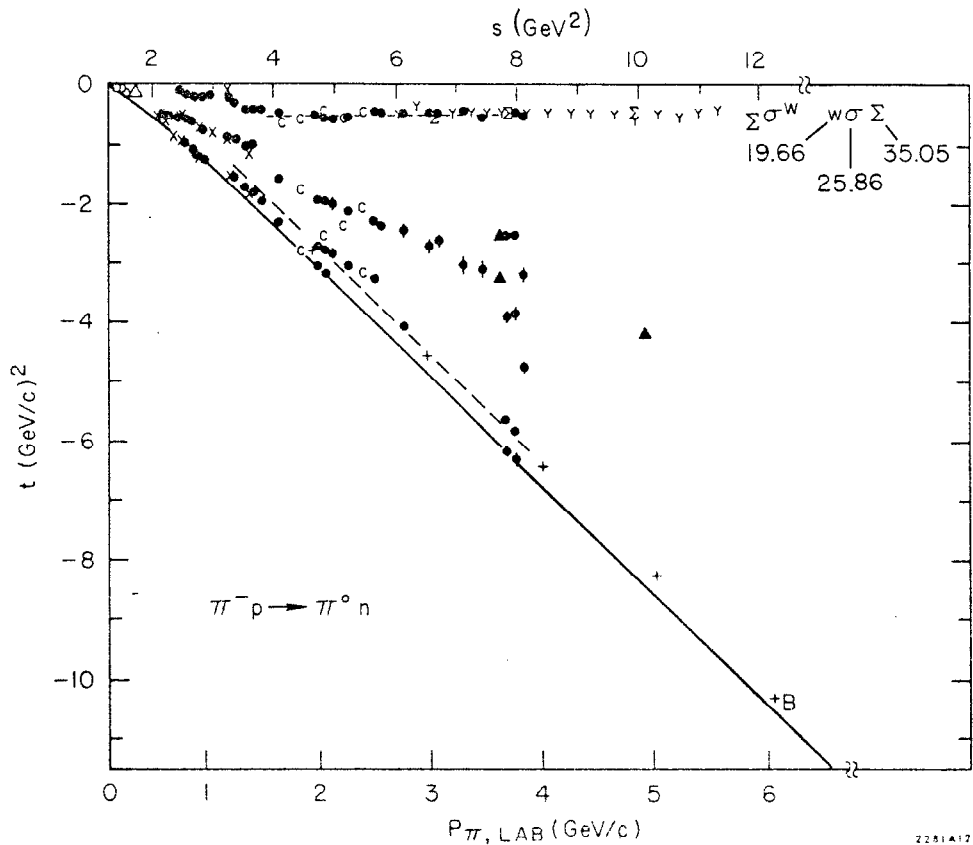
Fig. 8. Mandelstam plane plot of the minima in the differential
cross section for $\pi^-p \to \pi^0 n$.

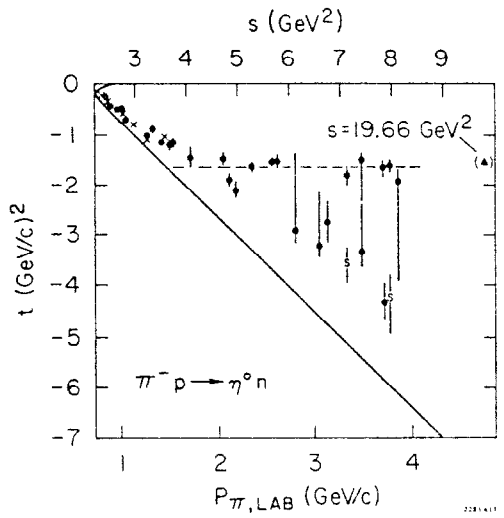Fig. 9. Mandelstam plane plot of
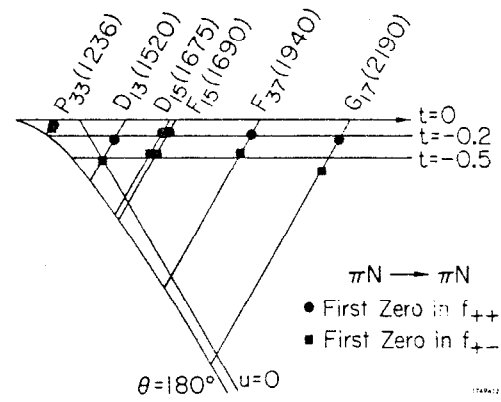the minima in the differential cross
section for $\pi^-p \to \eta^0 n$.

Fig. 10. Location of the first zero
in the contribution of prominent
resonances to the s-channel helicity
amplitudes for πp scattering.

For K⁻p scattering a more complete separation[27] has been done yielding s channel helicity amplitudes with definite t channel isospin I_t=0,1. The results are shown in Fig. 11. For the I_t=0 helicity nonflip amplitude, and the I_t=1 helicity flip amplitude, the fixed t zero structures at $-t \sim 0.2$ GeV^2 and $-t \sim 0.5$ GeV^2 respectively, are again observed. The other two amplitudes are smaller in magnitude than the first two mentioned (cf. Fig. 6), thus the random structure of zeros in these results, Fig. 11b,c, may only reflect uncertainties in the analysis and in the resonance parameterizations used.

The data suggest therefore that: (a) zeros or pronounced minima occur at values of momenta transfer that change only slowly, if at all, with beam momentum; and (b) several of these features exist virtually from reaction threshold to the highest energies presently measured. We note that these results also carry over to $\pi\pi$ scattering where recent analyses[28] reveal similar fixed t zero structures in $\pi\pi$ amplitudes with well defined t channel isospin.

Polarization changes with energy

In channels with one t channel exchange, or with two exchanges thought to be exchange degenerate (EXD) polarization provides a possible means to observe different relative energy dependences of helicity flip and nonflip amplitudes (see Eq. (5)). For example, a large class of absorption models modify or "absorb" the nonflip amplitude to a much greater extent than the flip amplitude. If the absorption is then energy dependent, the nonflip amplitude will vary with energy more rapidly than the helicity flip amplitude, resulting in possible changes in the polarization.

To determine the energy trends in the data, polarization results for the reactions $\pi^- p \to \pi^0 n$,[29] $\bar{K}^0 p \to \pi^+ \Lambda^0$,[30] and $\pi^+ p \to K^+ \Sigma^+$,[31] are plotted in Fig. 12
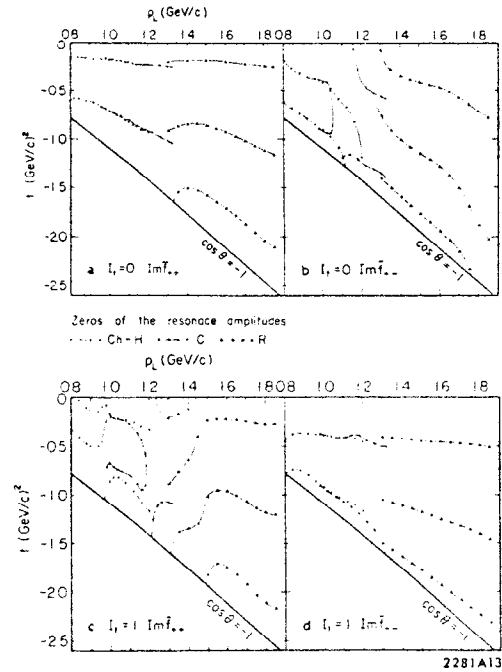

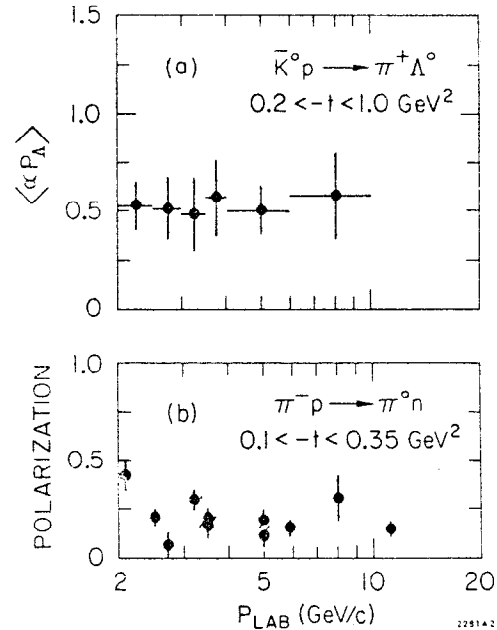Fig. 11. Location of zeros in the imaginary parts of the s channel helicity amplitudes for K⁻p scattering.

Fig. 12. Polarization data plotted as a function of beam momentum.
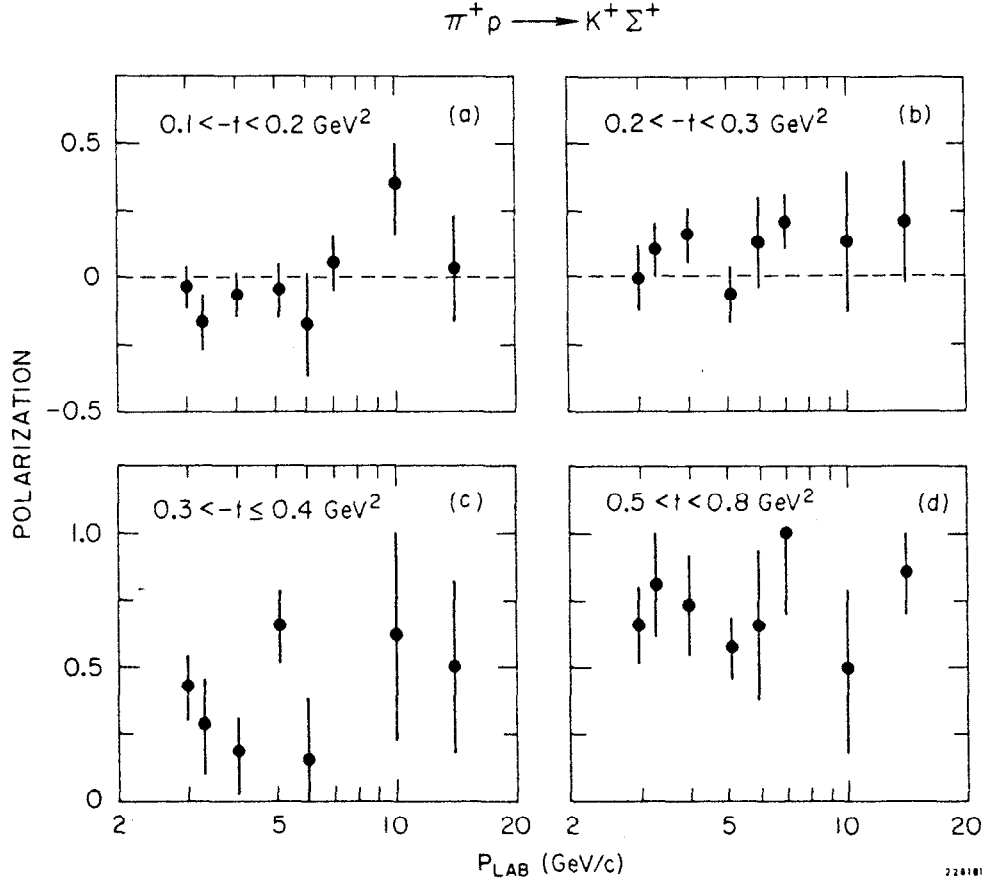
$$\pi^+ p \longrightarrow K^+ \Sigma^+$$

Fig. 13. Polarization data for $\pi^+ p \rightarrow K^+ \Sigma^+$ plotted as a function
of momentum transfer and beam momentum.

and Fig. 13 for beam momenta $\gtrsim 2$ GeV/c. Momentum transfer intervals
are chosen where the polarization is only slowly varying in t. The data are
observed to be consistent with little or no energy dependence. This suggests
therefore that helicity flip and nonflip amplitudes have similar energy de-
pendences in the momentum interval ~ 2 GeV/c to ~ 14 GeV/c.

Phases of the amplitudes at t=0

Although amplitude analyses typically require a prohibitive experimental
effort, this is not the case at t=0 for many pseudoscalar-meson baryon scat-
tering reactions. That is, the magnitude of the helicity nonflip amplitude is
obtained directly from the forward differential cross section, and the imagi-
nary part of the amplitude is provided by the optical theorem, for example:

$$\mathrm{Im}\ (\pi^- p \rightarrow \pi^0 n) = - \frac{k}{4\sqrt{2}\pi} \left(\sigma^T_{\pi^- p} - \sigma^T_{\pi^+ p} \right)$$

and

(6)

$$\mathrm{Im}(K^0_L p \rightarrow K^0_S p) = - \frac{k}{8\pi} \left(\sigma^T_{K^- n} - \sigma^T_{K^+ n} \right)$$

Recent results for the phase of the forward amplitude for $K_L^0 p \to K_S^0 p$,[32] are shown in Fig. 14. The data are consistent with having a constant phase, $\phi = -133.4 \pm 3.3^\circ$, over the momentum interval 1.5 to 50 GeV/c, in remarkable agreement with the naive Regge model prediction, $\phi = -135^\circ$ for $\alpha_\omega(0) = 0.5$. The curves on the figure result from using the optical theorem:

$$\phi = -\tan^{-1}\left\{\left[\left(\frac{\left(\frac{d\sigma}{dt}\right)_0}{\left(\frac{d\sigma}{dt}\right)_{optical}} - 1\right)^{-\frac{1}{2}}\right]\right\} \quad (7)$$

and parameterizing the data with the power law form:

$$\left(\frac{d\sigma}{dt}\right) = A \, p_{lab}^{-n}$$

The solid and shaded curves compare the phases of the forward amplitudes for $K_L^0 p \to K_S^0 p$ and $\pi^- p \to \pi^0 n$,[33] respectively. The uncertainties in the curves are $\sim \pm 6^\circ$ for $\pi^- p \to \pi^0 n$ and $\sim \pm 8^\circ$ for $K_L^0 p \to K_S^0 p$.

If the phases of the forward amplitudes are in approximate agreement with the Regge phase, then equal forward cross sections should be observed for those processes related by s-u crossing and dominated by EXD t channel exchanges.[34] Near equality of the t=0 cross sections is in fact observed in the channels $\pi p \to K\Sigma$ and $\bar{K}p \to \pi\Sigma$,[35] see Fig. 15, as well as for Kp charge exchange[36] and $\pi p \to K\Lambda$, $\bar{K}p \to \pi\Lambda$ data.[35]

In summary it is observed that: (a) the forward phase for $K_L^0 p \to K_S^0 p$ is consistent with being energy independent; and (b) the phases of the amplitudes at t=0 are consistent with simple Regge predictions.

Shrinkage

Using the parameterizations
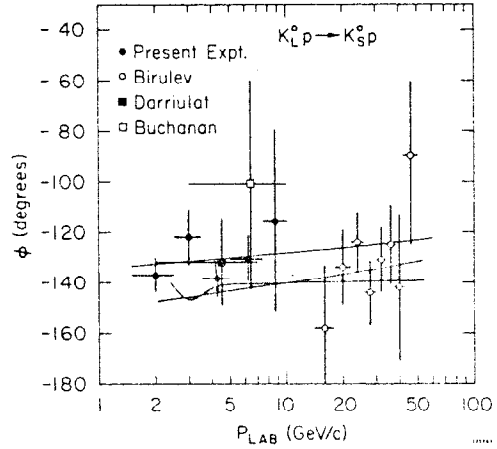
$$\frac{d\sigma}{dt} \propto e^{b(s)t} \quad (8)$$

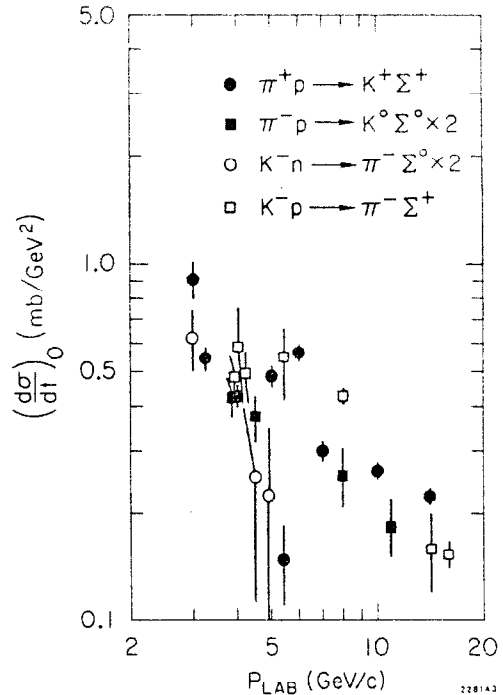Fig. 14. Phase of the scattering amplitudes at t=0 for the process $K_L^0 p \to K_S^0 p$.

Fig. 15. Differential cross sections at t=0 for the reactions $\pi p \to K\Sigma$ and $\bar{K}p \to \pi\Sigma$.

or

$$\frac{d\sigma}{dt} \propto P_{lab}^{2\alpha(t)-2} \qquad (9)$$

the energy dependence of the scattering amplitudes can be studied as a function of momentum transfer. A recent Serpukhov result for $\pi^-p \to \pi^0n$ is shown along with previous data[37] in Fig. 16. The curve in the figure represents the simple Regge prediction, $\alpha'=1$, approximately normalized to the data below 20 GeV/c. The Serpukhov data is interesting and may suggest that shrinkage has stopped by ~ 20 GeV/c. However, the evidence is not yet overwhelming.

At lower energies we obtain the effective Regge trajectory, $\alpha_{eff}(t)$, shown in Fig. 17 for the SLAC $K_L^0p \to K_S^0p$ data,[32] and for the reaction $\pi^-p \to \pi^0n$.[38] The solid curve in the figure gives the canonical ρ, ω trajectory $\alpha(t) = 0.5 + t$.

The $K_L^0p \to K_S^0p$ and $\pi^-p \to \pi^0n$ data (Fig. 17) do show shrinkage, $\alpha = \alpha(t)$, however

$$\alpha_{K_L^0p \to K_S^0p} < \alpha_{\pi^-p \to \pi^0n}$$

for $-t \lesssim 0.4$ GeV^2. Analogous differences are also found between the energy dependences of the reactions $\bar{K}p \to \pi\Lambda$ or $\pi p \to K\Lambda$ and the related Σ reactions, $\bar{K}p \to \pi\Sigma$ or $\pi p \to K\Sigma$.[24,30]

Simple Regge models would erroneously predict similar energy dependences for $K_L^0p \to K_S^0p$ and $\pi^-p \to \pi^0n$ reactions, and for Λ and Σ reactions. By contrast, it was observed in the previous section that the phases of the forward amplitudes were in good agreement with simple Regge predictions. For example, the $K_L^0p \to K_S^0p$ data[32] yield $\alpha_{eff}(0) = 0.48 \pm 0.04$ as determined from the phase of the forward amplitude, but $\alpha_{eff}(0) = 0.30 \pm 0.03$
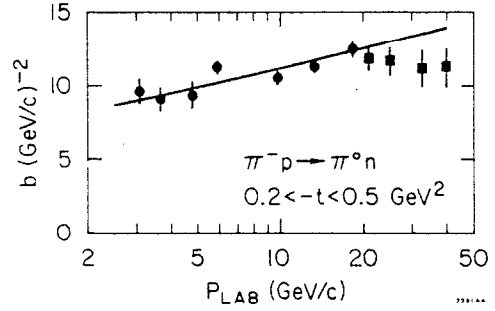

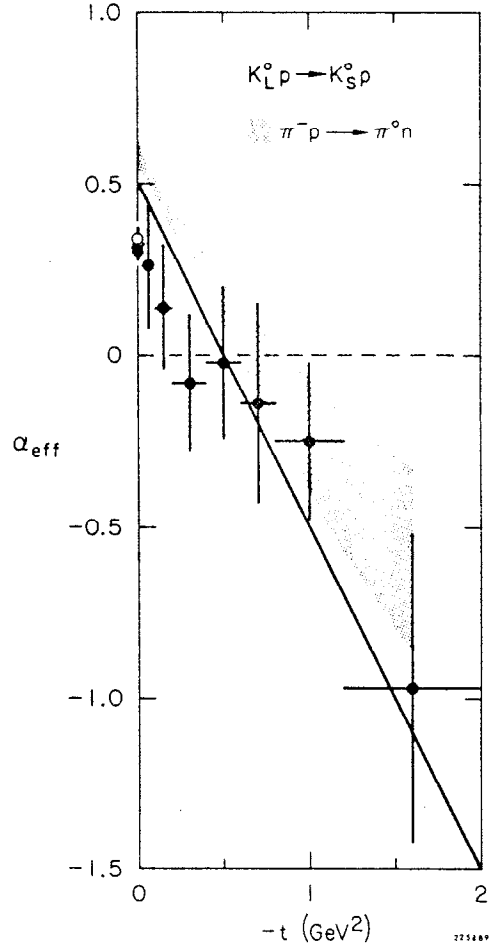Fig. 16. Slope parameter for the reaction $\pi^-p \to \pi^0n$.

Fig. 17. Energy dependence of the process $K_L^0p \to K_S^0p$; $\pi^-p \to \pi^0n$ data[38] is shown shaded in the figure.

from the energy dependence of the forward cross sections (see Fig. 17). The Regge model relationship between the phase and the energy dependence of the scattering amplitudes fails therefore at t=0; a similar conclusion for the helicity nonflip amplitude at momentum transfers -t > 0 can be inferred from the πp amplitude analyses at 6 GeV/c.[20,21]

Cross sections at t=0

In factorizable models (see for example Table II) the reactions $\pi^- p \to \pi^0 n$ and $K_L^0 p \to K_S^0 p$ are related by a single constant, assuming ρ and ω exchange amplitudes have similar energy dependences. This prediction disagrees with the data, as discussed in the last section; the magnitude of the discrepancy is observed by comparing the forward cross sections in Figs. 18 and 19.[32] An analogous comparison can be made using total cross section differences;[39] where $\pi^- p \to \pi^c n$ is replaced by

$$\Delta\sigma_{\pi^\pm p} = \sigma^T_{\pi^- p} - \sigma^T_{\pi^+ p}$$

and

$$K_L^0 p \to K_S^0 p \quad \text{by} \quad \Delta\sigma_{K^\pm p}$$

(see Eq. (6)). The results are shown in Fig. 20. Again the Kp data are observed to decrease with energy more rapidly than the πp data.

One conclusion is that ω and ρ exchanges, dominating $K_L^0 p \to K_S^0 p$ and $\pi^- p \to \pi^0 n$ respectively, are just intrinsically different. Alternatively, the comparison of forward $K_L^0 p \to K_S^0 p$ and Kp charge exchange cross sections[40] shown in Fig. 21 reveals that the magnitudes of the cross sections (pure coincidence?) as well as their momentum dependence are in excellent agreement. This result suggests that the t channel exchanges in these processes (ρ, ω, A_2) are consistent with EXD, and that direct channel effects cause the disagreement in the energy dependences

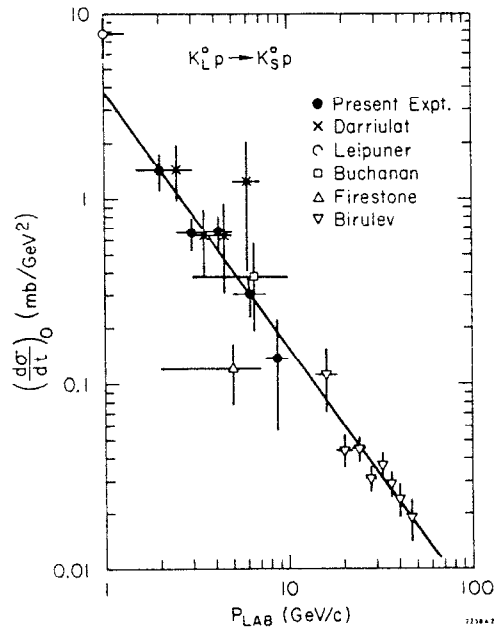Fig. 18. Differential cross sections at $t = 0$ for the reaction $K_L^0 p \to K_S^0 p$.

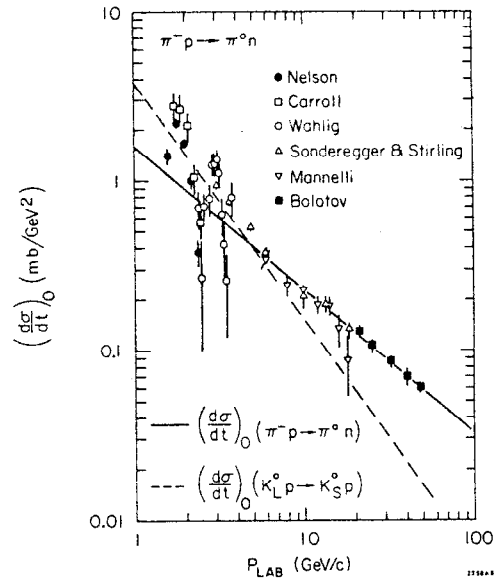Fig. 19. Differential cross sections at $t = 0$ for $\pi^- p \to \pi^0 n$; the solid curve is a power law fit to the data above 5 GeV/c, the dashed line represents the forward cross sections for $K_L^0 p \to K_S^0 p$.
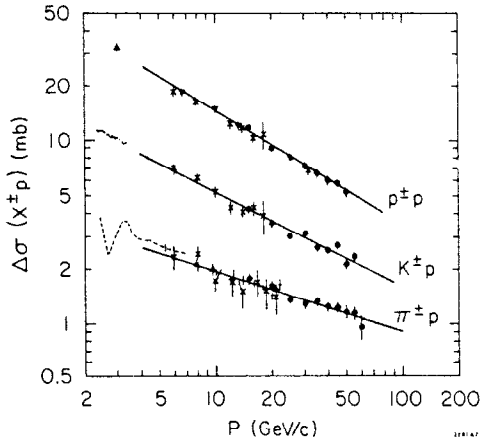
Fig. 20. Differences of total cross sections.

Fig. 21. Differential cross sections at $t = 0$ for the reactions $K^-p \rightarrow \bar{K}^0n$ and $K^+n \rightarrow K^0p$; the dashed line represents the forward cross sections for $K_L^0p \rightarrow K_S^0p$.

of the $K_L^0p \rightarrow K_S^0p$ and $\pi^-p \rightarrow \pi^0n$ forward cross sections.

To check this conjecture we note that the extrapolated $K^-p \rightarrow \bar{K}^0n$ cross section, Fig. 21, provides an upper bound to the total cross section difference $K^-N = \sigma_{K^-p}^T - \sigma_{K^-n}^T$, shown as the solid curve on the "K^-N" data in Fig. 22. The curve falls below the Serpukhov data, suggesting that the Kp charge exchange cross section should infact lie above the $K_L^0p \rightarrow K_S^0p$ cross section at momenta $\gtrsim 20$ GeV/c. However, negative values for the Serpukhov "K^+N" cross section differences, Fig. 22, disagree with lower energy data (and with duality)[41] suggesting that small systematic effects in the total cross sections may be causing problems in these cross section differences.

Thus, if ρ and ω trajectories are assumed EXD, simple t channel factorization is in disagreement with the $K_L^0p \rightarrow K_S^0p$ and $\pi^-p \rightarrow \pi^0n$ data. The comparison of $K_L^0p \rightarrow K_S^0p$ and Kp charge exchange data then suggest that factorization is infact broken by direct channel effects.[42]

Fig. 22. Differences of total cross sections for the reactions $K^-p - K^-n$ and $K^+p - K^+n$.

IV. SUMMARY

Our approach in this talk was first to indicate that absorption or direct channel effects are important in scattering reactions, then to systematically
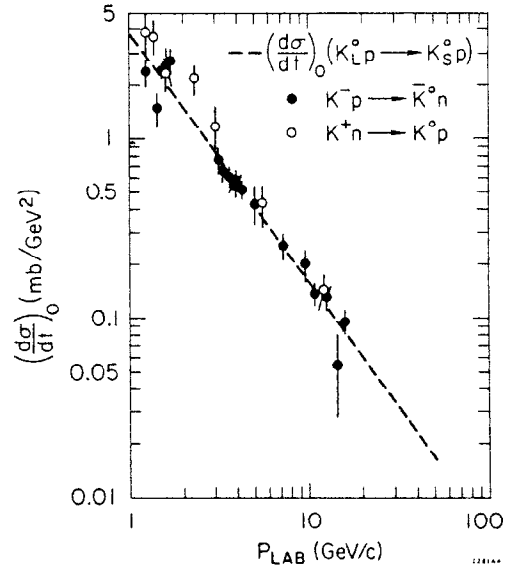
investigate energy trends in the data. This latter study presented evidence for disagreements with t channel factorization, and we conjectured that this was additional evidence for direct channel effects.

Generally, the energy trends in the data are consistent with shrinkage of the forward differential cross sections, but indicate that many features are essentially energy independent:

(a) the positions of minima in the differential cross sections;

(b) the location of zeros in the imaginary parts of some s channel helicity amplitudes; and

(c) the polarization, and phase of the t=0 scattering amplitude for those reactions with a limited number of possible exchanges in the t channel.

These observations provide qualitative as well as quantitative constraints on the energy dependence of the actual scattering amplitudes.

The pseudoscalar-meson baryon scattering results suggest that similar features may also exist in the $\pi\pi(K\pi)$ scattering amplitudes. For example, although amplitude zeros have been used in selecting phase shift solutions, our present observations suggest that approximately <u>fixed t</u> zeros occur in those amplitudes isolating a known meson exchange in the t channel. Similarly the observed energy independence of the phase of the forward meson-baryon scattering amplitudes may provide a guide in selecting $\pi\pi(K\pi)$ phase shift solutions at relatively high mass. Finally, the different direct channel effects in πp and Kp data indicate that π extrapolations may have different characteristics in $\pi\pi$ and $K\pi$ analyses, and perhaps also in analyses at different $\pi\pi$ or $K\pi$ masses.

V. ACKNOWLEDGEMENTS

REFERENCES

1. A. M. Boyarski et al., Phys. Rev. Letters 20, 300 (1968).
2. M. B. Davis et al., Phys. Rev. Letters 29, 139 (1972).
3. J. G. Lee et al., Nucl. Phys. B52, 292 (1973).
4. F. Bulos et al., Phys. Rev. Letters 26, 1453 (1971).
5. F. Henyey, G. L. Kane, J. Pumplin and M. H. Ross, Phys. Rev. 182, 1579 (1969).
6. A. B. Wicklund et al., Phys. Rev. Letters 29, 1415 (1972).
7. M. Davier and H. Harari, Phys. Letters 35B, 239 (1971).
8. K. Gottfried and J. D. Jackson, Nuovo Cimento 34, 735 (1964).
9. G. L. Kane, Experimental Meson Spectroscopy, ed. C. Baltay and A. H. Rosenfeld (Columbia University Press, New York, 1970).
10. P. Baillon et al., Phys. Letters 35B, 453 (1971).

11. G. Gayer et al., "$\pi\pi$ phase shifts, amplitude analysis and vector dominance test in the ρ-region of $\pi^-p \to \pi^-\pi^+n$ at 17.2 GeV/c" CERN preprint (1972).
12. P. K. Williams, Phys. Rev. 181, 1963 (1969).
13. G. Fox, Argonne Workshop on Meson Spectroscopy (1971).
14. M. Ross, F. S. Henyey and G. L. Kane, Nucl. Phys. B23, 269 (1970);
    H. Harari, Ann. Phys. (N.Y.) 63, 432 (1971);
    J.A.J. Matthews, Proceedings of Canadian Institute of Particle Physics
    Summer School, ed. R. Henzi and B. Margolis (McGill University Press,
    Montreal, 1972).
15. P. Estabrooks and A. D. Martin, Phys. Letters 41B, 350 (1972).
16. J.A.J. Matthews et al., Nucl. Phys. B32, 366 (1971);
    Y. Williamson et al., Phys. Rev. Letters 29, 1353 (1972);
    W. Michael and G. Gidal, Phys. Rev. Letters 28, 1475 (1972);
    P. Estabrooks and A. D. Martin, Phys. Letters 42B, 229 (1972);
    R. Diebold, private communication.
17. S. Barish and W. Selove, private communication.
18. J. M. Scarr and K.-W. Lai, Phys. Rev. Letters 29, 310 (1972).
19. The presence of a confirmed dip in ρ_{00}^H $d\sigma/dt$ at several incident momenta would presumably rule out background as an explanation.
20. P. Johnson et al., Phys. Rev. Letters 30, 242 (1973).
21. G. Cozzika et al., Phys. Letters 40B, 281 (1972).
22. A. D. Martin and C. Michael, Phys. Letters 37B, 513 (1971);
    F. D. Gault, H. F. Jones and M. D. Scadron, Nucl. Phys. B51, 353
    (1973); E. Fischback, M. M. Nieto, H. Primakoff and C. K. Scott,
    Phys. Rev. Letters 29, 1046 (1972).
23. C. Michael, 16th International Conference on High Energy Physics,
    CERN preprint REF. TH 1567-CERN (1972).
24. A. C. Irving, A. D. Martin and V. Barger, "Analysis of data for hypercharge exchange reactions," CERN preprint REF. TH 1585-CERN (1972).
25. R. K. Yamamoto et al., "Negative pion charge exchange and η^0 production from 1.3 to 3.9 GeV/c," MIT preprint (1972).
26. H. Harari, SLAC preprint SLAC-PUB-837 (1970).
27. M. Fukugita and T. Inami, Nucl. Phys. B44, 490 (1972).
28. M. Pennington, "$\pi\pi$ amplitudes, structure and zeros," International
    Conference on $\pi\pi$ Scattering and Associated Topics, Tallahassee (1973).
29. P. Bonamy et al., Nucl. Phys. B16, 335 (1970);
    D. D. Brobnis et al., Phys. Rev. Letters 20, 274 (1968);
    P. Bonamy et al., Amsterdam International Conference on Elementary
    Particles (1971); D. Hill et al., Phys. Rev. Letters 30, 239 (1973).
30. R. J. Yamartino, Ph.D. thesis, Stanford University (1973).
31. S. M. Pruss et al., Phys. Rev. Letters 23, 189 (1969);
    A. Bashian et al., Phys. Rev. D4, 2667 (1971).
32. G. W. Brandenburg et al., to be published.
23. G. Höhler and R. Strauss, "Tables of pion-nucleon forward amplitudes,"
    Karlsruhe preprint (1971).
34. F. J. Gilman, Phys. Letters 29B, 673 (1969).
35. J. S. Loos and J.A.J. Matthews, Phys. Rev. D6, 2463 (1972).
36. D. Cline, J. Matos, and D. D. Reeder, Phys. Rev. Letters 23, 1318
    (1969).
37. V. N. Bolotov et al., "A study of $\pi^-p \to \pi^0n$ charge-exchange in the
    momentum range 20 to 50 GeV/c," Serpukhov preprint (1972);

P. Sonderegger et al., Phys. Letters 20, 75 (1966);

A. V. Stirling et al., Phys. Rev. Letters 14, 763 (1965).

38. G. Höhler, J. Baacke, H. Schlaile and P. Sonderegger, Phys. Letters 20, 79 (1966).

39. S. P. Denison et al., "Differences of total cross sections for momenta up to 65 GeV/c," Serpukhov preprint (1972).

40. A. A. Hirata et al., Nucl. Phys. B30, 157 (1971);

M. Aguilar-Benitez, R. L. Eisner and J. B. Kinson, Phys. Rev. D4, 2583 (1971);

I. Butterworth et al., Phys. Rev. Letters 15, 734 (1965);

C. G. Wohl, Ph.D. thesis UCRL-16288 (1965);

Y. Goldschmidt-Clermont et al., Phys. Letters 27B, 602 (1968);

L. Moscoso et al., Phys. Letters 32B, 513 (1970);

P. Astbury et al., Phys. Letters 23, 396 (1966);

D. Cline, J. Penn and D. D. Reeder, Nucl. Phys. B22, 247 (1970);

A. Firestone et al., Phys. Rev. Letters 25, 958 (1970);

G. C. Mason and C. G. Wohl, "Reactions $K^-p \rightarrow \bar{K}^0 n$, $K^-p \rightarrow \Lambda \pi^0$ and $K^-p \rightarrow \Lambda \eta$ at 3.13, 3.30, and 3.59 GeV/c," Oxford University preprint (1973);

R. Blokzijl et al., Nucl. Phys. B51, 535 (1973);

R. J. Miller et al., "Two body final states in K^-p interactions at 14.3 GeV/c," Rutherford preprint RPP/H/102 (1972);

E. H. Willen et al., "High energy differential cross sections for K^0 production," BNL preprint BNL 16681 (1972).

41. H. Harari, Phys. Rev. Letters 20, 1395 (1968);

P.G.O. Freund, ibid 20, 235 (1968).

42. The explanation for the difference in the energy trends of the forward cross sections for $K_L^0 p \rightarrow K_S^0 p$ and $\pi^- p \rightarrow \pi^0 n$ is not clear, however. Typically absorption models correct simple Regge predictions in proportion to the total cross sections of the particles involved. However, $\sigma_{Kp}^T < \sigma_{\pi p}^T < \sigma_{pp}^T$ in contrast to the energy dependences of the data, see Fig. 20, where $\Delta\sigma_{pp}$ and $\Delta\sigma_{Kp}$ data are quite similar, and substantially different from the energy dependence of the $\Delta\sigma_{\pi p}$ data. Similar problems arise in discussing the difference in energy dependence of the channels $\bar{K}p \rightarrow \pi\Lambda$ and $\bar{K}p \rightarrow \pi\Sigma$.